# Distributed Control for Bending Propulsion Mechanism in Water*

Shunichi KOBAYASHI**, Akira SEKIZUKA***,
Toshifumi OKUNISHI*** and Hirohisa MORIKAWA**

In this paper we describe the distributed controls for an ultra-multilink bending propulsion mechanism in water. Functions of the neural oscillator of an organism were programmed into each unit that consists of a controller and an actuator. The bending movement was generated by the cooperation of each unit. As an experiment of robustness, we assumed the case of a locked joint (no rotation). The bending movement was recovered using the cooperation of other joints. We discussed the influence of movement of the mechanism on thrust force.

***Key Words***: Distributed Control, Bending Movement, Propulsion, Robustness, Robotics

## 1. Introduction

Since organisms are fairly autonomic, functional and efficient, the study of machines modeled on the motions of organisms is very significant in the engineering field. Most propulsion mechanisms of organisms in water employ alternative movements of fins and bending movements of the body. From this point of view, we observed organisms that swim in water by bending motions, and developed an ultra-multilink bending propulsion mechanism to reproduce the bending motion behavior of the organisms[1]. Motors on the joints in this mechanism were controlled by a personal computer as the concentrated control. However, as the number of motors in the mechanism increased, the amount of calculation for control also increased. Hence, it tends to be difficult to control various flexible movements. For concentrated control of large scale complicated systems, it is difficult to maintain high speed, robustness, flexibility and extensiveness. One solution to this problem, is the autonomous distributed system theory. In the autonomous distributed system, the entire system keeps a harmony and achieves its aim effectively while each element obeys its own individual rule. For that purpose, each element should be autonomous and cooperative[2].

On the other hand, the control systems for the motion of organisms that swim in water are the original forms for autonomous distributed control systems[3]. For example, larvae of crayfish have five pairs of legs in the abdominal region, and swim by an alternative movement of each pair of legs with a phase delay from posterior side to anterior side. The five pairs of legs are controlled by five pairs of assembly of nerve cells in the abdominal region. Each assembly of nerve cells acts as a function of the neural oscillator. The phase relation is controlled by the interaction among the assemblies of nerve cells. Leeches swim by generating vertical waves from head to tail, contracting the abdomen and the back of each segment alternately, and keeping a phase difference between neighboring segments. It is thought that distributed nerve oscillators along the nerve cord in abdomen control the contraction of the muscles. Therefore, this control method can be applied for the bending propulsion mechanism in water.

Hirose and Takanashi applied the distributed control of long (high aspect ratio) locomotive robots that consist of many actuators[4],[5], and Yuasa and Ito carried out computer simulation to generate swimming patterns of organism using the distributed autonomous control system[6]. However, no experimental studies are available on distributed control for long swimming robots, which consists of many actuators.

* Received 5th July, 2000. Japanese original: Trans. Jpn. Soc. Mech. Eng., Vol. 65, No. 633, C (1999), pp. 1886-1891 (Received 12th February, 1998)

** Department of Functional Machinery and Mechanics, Faculty of Textile Science and Technology, Shinshu University, 3-15-1 Tokida, Ueda, Nagano 386-8567, Japan. E-mail: shukoba@giptc.shinshu-u.ac.jp

*** Graduate School of Science and Technology, Shinshu University, 3-15-1 Tokida, Ueda, Nagano 386-8567, Japan

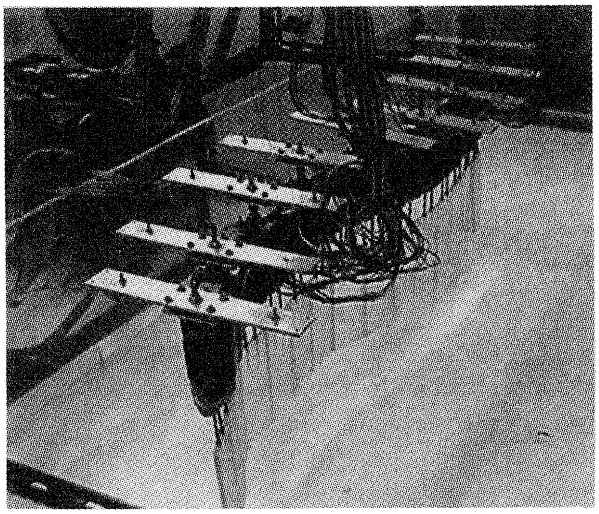

Fig. 1 Photograph of bending propulsion mechanism

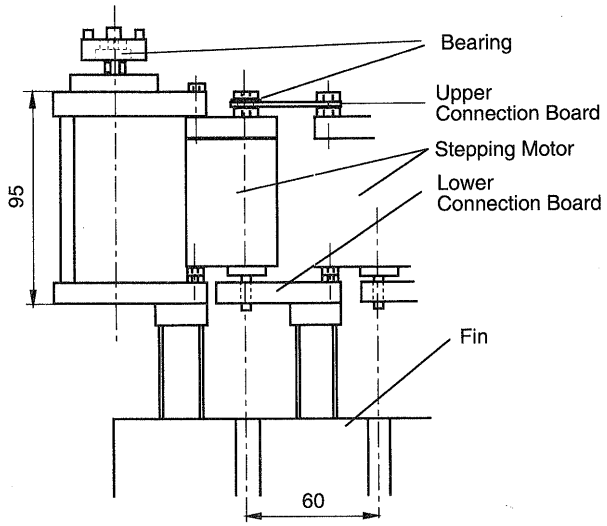


Fig. 2 Details of bending mechanism

We have developed a distributed control system for an ultra-multilink bending propulsion mechanism in water (hereinafter called the "bending propulsion mechanism"), and carried out two experiments: (1) First, the function of nerve oscillator of the organism is installed in each controller. We generate the entire bending movement pattern by a cooperative control system that adjusts the phase difference between neighboring controllers, and discuss the thrust force characteristics. (2) Second, as the robustness test, we assume the case of one locked joint (no rotation). We discuss the thrust force characteristics while the other joint recovers to maintain the entire bending motion.

## 2. Bending Propulsion Mechanism in Water and the Control System

### 2.1 Construction of the bending propulsion mechanism

The photograph of the bending propulsion mechanism, the details of bending mechanism and the experimental setup are shown in Figs. 1, 2 and 3. The actuators consist of 15 stepping motors with reduction gearboxes (hereafter termed "motors"). The rotation of the shaft drives the lower connection board, and generates the bending movement with an adjacent lower connection board. To immerse the fin in the water, the bending propulsion mechanism is hung by nylon strings from the inner frame. To increase the degree of freedom of the bending propulsion mechanism from the inner frame, springs are attached to the nylon strings, and bearings are placed on the connecting part of the bending propulsion mechanism with nylon strings. The full length of the bending propulsion mechanism and the number of motors are 960 mm and 15, respectively.

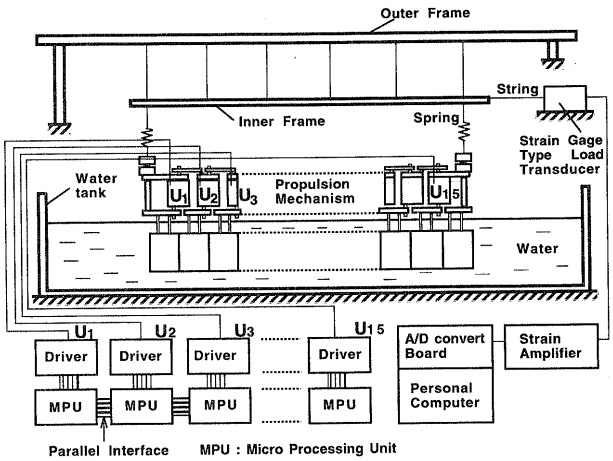


Fig. 3 Experimental setup

### 2.2 Control of the bending propulsion mechanism

We used the distributed control by connecting each controller to each motor. Z 80 MPU boards are used as controller for this experimental system. A pair comprising a controller and actuator was termed as a "unit", and numbered from the top and termed $U_1$, $U_2$, $\cdots U_{15}$. Each unit communicates with the adjacent units through a parallel I/O port.

### 2.3 Measurement of thrust force

The total thrust force of the bending propulsion mechanism is measured by a strain-gage type load transducer (with computer) connected with a string to the inner frame. To measure the negative thrust force, an initial tension was given to the string while still in a stationary condition.

## 3. Generation of Bending Pattern of the Bending Propulsion Mechanism

### 3.1 Method of generation

We paid attention to the case of the swimming

pattern of an organism which was formed by the phase delay of each nerve oscillator along the nerve cord from head to tail. To generate the bending movement of the propulsion mechanism, each unit of the propulsion mechanism works as an oscillator with a constant phase delay from the anterior adjacent unit.

Each unit incorporates the programmed data of the periodic sinusoidal rotation angle variation as the oscillator, and the information of rotation speed (fast, normal and slow rotation modes) to be able to adjust the phase difference between the phase of its unit and that of the anterior adjacent unit. Each unit always confirms its phase and transmits it to the posterior adjacent unit. After an input of the trigger from outside the system, each unit $U_n$ starts to calculate the phase difference between its phase and the received phase of the anterior adjacent unit $U_{n-1}$, and selects the adequate rotation mode to bring the phase difference close to the target phase difference. Using this method, if the period of the top unit and the target phase difference are constant, after the input of trigger, the random phase differences are adjusted gradually to attain a constant value, and a bending wave will be formed from the top to the tail. The final converged wave is a discrete wave of a Serpenoid curve[4] of which the curvature changes sinusoidally along the longitudinal axis of the bending propulsion mechanism.

We measure the number of adjustment (fast or slow rotation) mode units $N_a$ after the input of trigger, and define the converge on the formation of bending wave as $N_a=0$. The time at the input of trigger is $t=0$ s. The periods of fast, normal and slow rotation modes are 3.13 s, 6.25 s and 9.38 s, respectively. In order to fix the number of waves at one, the target phase difference is set to $2\pi/16$. The period of converged bending movement is 6.25 s, which is equal to the period of normal rotation mode.

### 3.2 Results and discussion

Figure 4 shows the formation of a bending wave (centerline of bending propulsion mechanism). Figure 5 shows the number of adjustment (fast and slow rotation) mode units versus time. The results shown in both figures are dependent on the initial shape at $t=0$ s. To discuss the formation of bending wave with time, the initial shape was kept as a straight line. At the start of the movement, the form of the bending propulsion mechanism was an arched curve, and then a progressive wave of the bending movement was generated gradually, similar to the swimming form of a snake. As observed from Fig. 5, since all the phase differences are 0 at $t=0$ s, all units adjust to the target phase difference. Thus, the number of adjustment

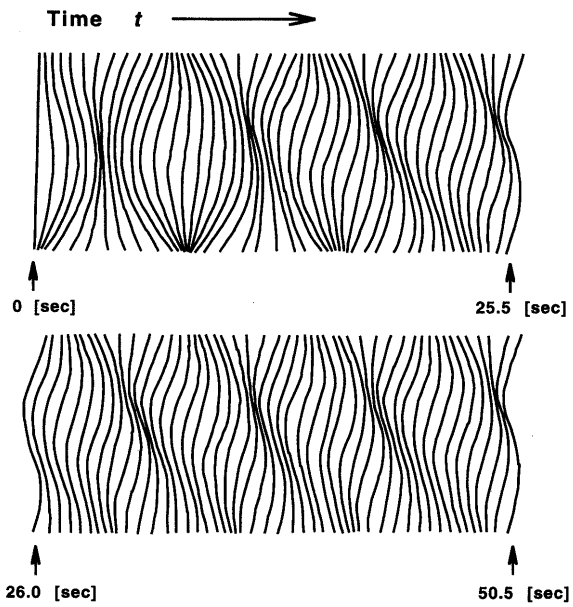


Fig. 4 Formation of bending wave

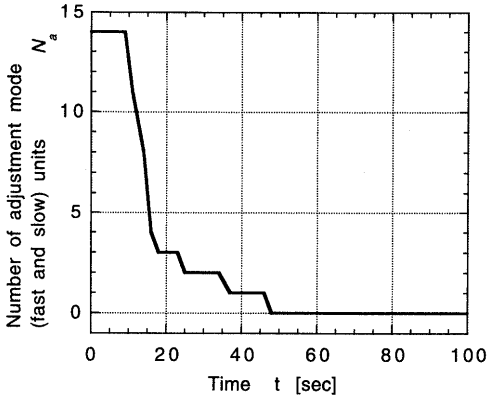


Fig. 5 Number of adjustment (fast and slow rotation) mode units versus time

(fast and slow rotation) mode units are reduced, and the converged bending movement is formed after approximately 50 s.

Figure 6 shows the mean thrust force and thrust force difference versus time. Mean thrust force ($F_{mean}$) and thrust force difference ($|F_{max}-F_{min}|$) are measured at 6.25 s (period of converged bending wave) intervals from $t=0$ s. $F_{mean}$ decreased at the beginning, but increased suddenly around 15 s, and then converged to about 0.15 N. $|F_{max}-F_{min}|$ increased for around 45 s, and then reduced to roughly 0.45 N. The large increase of $F_{mean}$ and $|F_{max}-F_{min}|$ was caused by the arched curve bending form. The variation of thrust force in one bending cycle is similar to the normal condition shown in Fig. 9.

## 4. Robustness of Bending Propulsion Mechanism

### 4.1 Method of robustness control

The robustness control in the case where the bending propulsion mechanism maintains the whole

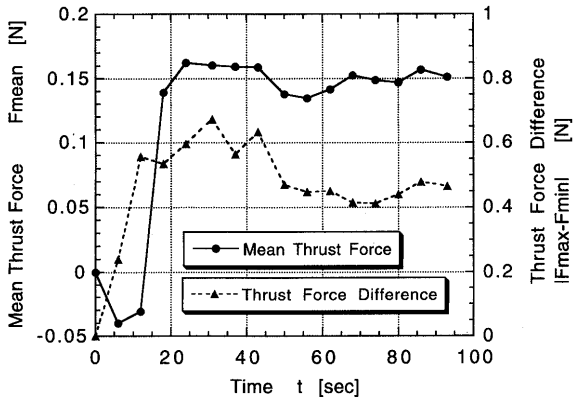


Fig. 6 Mean thrust force and thrust force difference versus time

bending movement while a joint of the unit is locked due to a problem or obstruction was carried out. We applied the algorithm proposed by Kobayashi et al.[7] for an ultra-multilink manipulator.

Each unit $U_n$ has the target position of the posterior the adjacent unit $U_{n+1}$, $\boldsymbol{p}_{n+1}(t_i)=(p_{n+1,x}, p_{n+1,y})$, where $t_i$ is the discrete time in one cycle. $U_n$ always moves to coincide with the position of $U_{n+1}$, $\boldsymbol{c}_{n+1}=(c_{n+1,x}, c_{n+1,y})$ to achieve the target position $\boldsymbol{p}_{n+1}(t_i)$ by the following equation,

$$\lim_{k\to\infty} \boldsymbol{c}_{n+1}(k)=\boldsymbol{p}_{n+1}(t_i), \tag{1}$$

where $k$ is the number of corrections to coincide $\boldsymbol{c}_{n+1}$ with $\boldsymbol{p}_{n+1}(t_i)$. Using this equation, the bending wave is formed. Actually, it is difficult to coincide the positions perfectly, because the time for correction is limited within the period of $t_{i+1}-t_i$. However, each unit can always move to follow the target position.

Figure 7 shows the coordinate system of a bending propulsion mechanism. Coordinate $\boldsymbol{c}_{n+1}$ of unit $U_{n+1}$ and coordinate $\boldsymbol{c}_1$ of the top unit $U_1$ are given by,

$$\begin{cases} \boldsymbol{c}_{n+1,x}(k)=\boldsymbol{c}_{n,x}(k)+L\cos\sum_{s=1}^{n}\theta_s(k) \\ \boldsymbol{c}_{n+1,y}(k)=\boldsymbol{c}_{n,y}(k)+L\sin\sum_{s=1}^{n}\theta_s(k) \end{cases} \tag{2}$$

$$\begin{cases} \boldsymbol{c}_{1,x}(k)=L \\ \boldsymbol{c}_{1,y}(k)=0 \end{cases} \tag{3}$$

where $L$ is link length and $\theta_s$ is the relative angle of $S$th unit. $U_n$ gets the coordinate of $U_n$ and the sum of relative angles from the anterior adjacent unit by communication, and calculates the position of $U_{n+1}$ following Eq.(2). The control law for reaching the position $U_{n+1}$, $\boldsymbol{c}_{n+1}$ to achieve the target position $\boldsymbol{p}_{n+1}$ is given as,

$$\begin{aligned} a_n(k)=&-d\cdot\mathrm{sgn}[\{\boldsymbol{p}_{n+1,x}(k)-\boldsymbol{c}_{n+1,x}(k)\} \\ &\times\{\boldsymbol{c}_{n+1,y}(k)-\boldsymbol{c}_{n,y}(k)\}-\{\boldsymbol{p}_{n+1,y}(k)-\boldsymbol{c}_{n+1,y}(k)\} \\ &\times\{\boldsymbol{c}_{n+1,x}(k)-\boldsymbol{c}_{n,x}(k)\}] \end{aligned} \tag{4}$$

$$\theta_k(k+1)=\theta_n(k)+a_n(k) \tag{5}$$

where $a_n(k)$ is the rotation angle of the motor and its sign indicates the rotation direction. $d$ is a single stepping angle of the motor. Following this control law, even if a unit has an accident but its functions of calculation and communication are working, an approximate bending wave is kept because the posterior side units approach their target positions as shown in Fig. 8. Consequently, the robustness of the bending propulsion mechanism is increased.

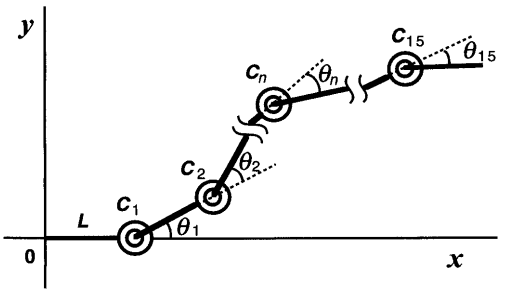


Fig. 7 Coordinate system of bending propulsion mechanism

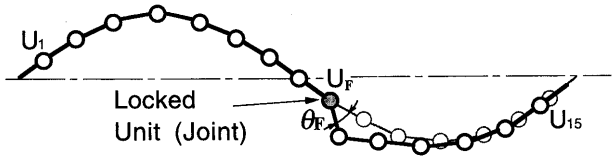


Fig. 8 Restoration of wave form

### 4.2 Results and discussion

In this study, we assumed the case of the problem where a joint of the unit which was locked was represented by the software, and discussed the influence of the thrust force on the position of the locked joint of the unit and its locked angle. The number of bending waves was one and the period of bending movement was 6.82 s.

Figure 9 shows the variations of thrust force during one bending cycle under normal conditions with no problems, $U_F=4$ ($U_4$ was locked) at 0 degree, and $U_F=12$ ($U_{12}$ was locked) at 0 degree. This figure indicates that the variation in the first half cycle is greater for $U_F=4$ (a unit of anterior side is locked).

Figure 10 shows the relationship between the position of locked unit $U_F$ and mean thrust force in one bending cycle $F_{\mathrm{mean}}$. In the case that a unit is locked, the mean thrust force is reduced to half that in the normal condition, but is still positive. Hence this distributed control has the function of robustness. In the case where $U_F=1$ (top unit is locked), the locked angle $\theta_F$ influences the mean thrust force.

Figure 11 shows the relationships between the position of locked unit $U_F$ and thrust force difference $|F_{\max}-F_{\min}|$. In the case where a posterior side unit is locked, there is no difference between this case and that under normal conditions. However, in the case

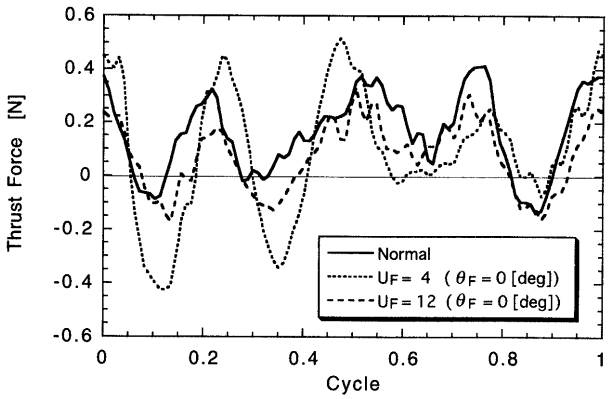


Fig. 9 Variation of thrust force during one bending cycle

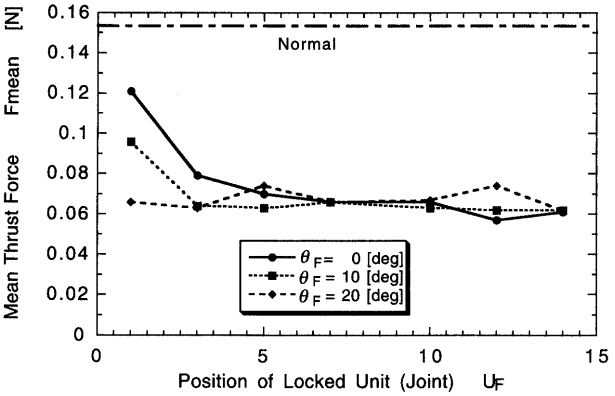


Fig. 10 Relationships between position of locked unit and mean thrust force

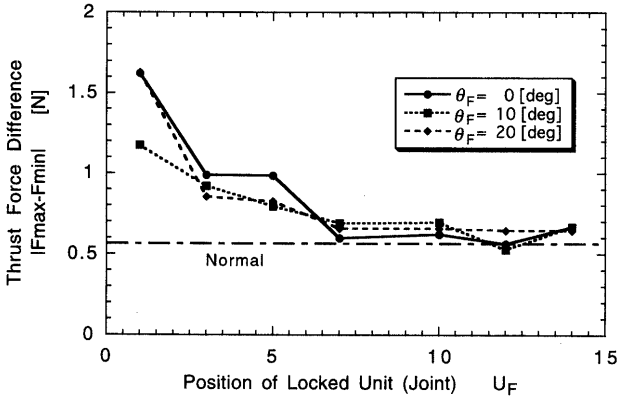


Fig. 11 Relationships between position of locked unit and thrust force difference

where an anterior side unit is locked, the thrust force difference increases. This can be explained in terms of the increase in the number of adjusting units that move to coincide with the target positions, and this increase affects the smooth bending wave.

We attempted the same experiment under non-robust control conditions. The bending wave was lost, and extremely high torque was loaded onto the unit and it went out of control. Hence we could not carry out the comparison between the robust control and the non-robust control conditions.

## 5. Conclusions

We developed a distributed control system of ultra-multilink propulsion mechanism in water, and carried out two experiments. The following results were obtained.

(1) The function of the nerve oscillator of an organism was installed in each controller. As the result of cooperative control using the adjustment of the phase difference between neighboring units, the whole bending movement pattern was generated and stable thrust force characteristics were obtained.

(2) As the robustness test, we assumed the case of a locked unit (no rotation). The whole bending movement was achieved by the recovery of the other units. Although the mean thrust force was reduced it was still positive. Thrust force difference increased when an anterior side unit was locked.

Problems to be solved in the future include the following.

(1) Measurements of the thrust force and its normal component for each unit, along with the load torque of each motor.

(2) Definition and evaluation of thrust efficiency.

(3) Improvement of robustness: self-creation of bending motion in the case where a part of the unit is locked.

## References

(1) Kobayashi, S., Propulsion Force Characteristics of Propulsion Mechanism Imitating Bending-movement Organisms in Water, Trans. Jpn. Soc. Mech. Eng., (in Japanese), Vol. 60, No. 579, B (1994), pp. 3613-3617.

(2) Nagata, T., Ziritu Bunsan wo Mezasu Robot System, (in Japanese), (1995), pp. 1-15, Ohm Sha.

(3) Suzuki, R., Seitai ni Okeru Bunsan to Seigyo, (in Japanese), Journal of the Society of Instrument and Control Engineers of Japan, Vol. 26, No. 1 (1987), pp. 78-81.

(4) Hirose, S., Seibutu Kikai Kougaku, (in Japanese), (1987), pp. 112-116, Kogyo Chosakai

(5) Takanashi, N., Yashima, S. and Aoki, K., Complete Modular Links and its Application to a 3D Hyper Redundant Robot, (in Japanese), Proc. The 13th Annual Conf. of Robotics Society of Japan, (1995), pp. 499-500.

(6) Yuasa, H. and Ito, M., Ziritsu Bunsan System no Kyocho to Taiikiteki Chitsujyo Keisei, Journal of the Society of Instrument and Control Engineers of Japan, Vol. 29, No. 10 (1990), pp. 929-934.

(7) Kobayashi, H., Shimemura, E. and Suzuki, K., An Ultra-Multi Link Manipulator, IEEE/RSJ Int. Workshop on Intelligent Robots and Systems IROS '91, (1991), pp. 173-178.